

# We are IntechOpen, the world's leading publisher of Open Access books Built by scientists, for scientists

4,800

Open access books available

122,000

International authors and editors

135M

Downloads

Our authors are among the

154

Countries delivered to

TOP 1%

most cited scientists

12.2%

Contributors from top 500 universities



WEB OF SCIENCE™

Selection of our books indexed in the Book Citation Index  
in Web of Science™ Core Collection (BKCI)

Interested in publishing with us?  
Contact [book.department@intechopen.com](mailto:book.department@intechopen.com)

Numbers displayed above are based on latest data collected.  
For more information visit [www.intechopen.com](http://www.intechopen.com)



---

# **Delamination and Longitudinal Cracking in Multilayered Composite Nanostructured Coatings and Their Influence on Cutting Tool Wear Mechanism and Tool Life**

Alexey Vereschaka, Sergey Grigoriev,  
Nikolay Sitnikov, Gaik Oganyan,  
Anatoliy Aksenenko and Andre Batako

Additional information is available at the end of the chapter

<http://dx.doi.org/10.5772/intechopen.72257>

---

## **Abstract**

The wear and failure mechanism for multilayered nanostructured coatings has a number of significant differences from the one typical for monolithic single-layered coatings. In particular, while the strength of adhesion bonds at the “substrate-coating” boundary is important for monolithic coatings, then for multilayered nanostructured coatings, the strength of adhesion and cohesion bonds at interlayer boundaries and boundaries of separate nano-sublayers becomes of significant significance. Meanwhile, the delamination arising in the structure of multilayered nanostructured coatings can have both negative (leading to loss of coating uniformity and subsequent failure of coating) and positive influences (due to decrease of internal stresses and inhibition of transverse cracking). Various mechanisms of formation of longitudinal cracks and delaminations in coatings on rake tool faces, which vary based on the compositions and architectures of the coatings, are studied. In addition, the influence of internal defects, including embedded microdrops and pores, on the formation of cracks and delaminations and the failure of coatings is discussed. The importance of ensuring a balance of the basic properties of coatings to achieve high wear resistance and maximum tool life of coated metal-cutting tools is shown. The properties of coatings and the natures of their failures, as investigated during scratch testing and dry turning of steel C45, are provided.

**Keywords:** wear-resistant coatings, wear, crack, fracture, tool life, PVD coatings, delamination, nanoscale structures

## 1. Introduction

### 1.1. Background

Further increases in efficiency of machining and cutting speeds as well as tightening of reliability requirements associated with greater levels of automation of production result in the need to create new tool materials with enhanced performance characteristics. One way to improve the performance characteristics of tool materials is to enhance their surface properties by applying modified coatings [1]. In turn, the properties of modified coatings continue to be improved, and their architecture and elemental composition become more complicated. In particular, multilayered composite coatings, nanostructured and gradient coatings, and coatings with multicomponent elemental composition have been used extensively in recent years [2]. The use of a multilayered architecture of coatings and the use of nanostructured technology can significantly improve the performance characteristics of a new generation of coatings. However, along with the use of such coatings come new problems that did not occur with monolithic coatings of the first generation. In particular, problems arose concerning interlayer delamination and formation of specific longitudinal cracks in the structure of coating. A large number of studies examining problems of cracking have been conducted. The general assumption is that the formation of microcracks is associated with the displacement of dislocations [3–6]. A number of mechanisms for the formation of dislocation microcracks are well known [3, 4, 6]. In principle, those mechanisms provide for blocking of the progress of dislocation by some obstacle (e.g., a grain boundary, a boundary of nanolayers, or inclusion). If in some slip plane dislocations stop before a sufficiently powerful obstacle, then a cluster of dislocations is formed, and it causes a high concentration of stresses at the obstacle. This concentration of stresses results in formation of a dislocation microcrack. It should be noted that the problems of crack formation and delamination in the structures of multilayered coatings have not been studied as thoroughly as have other aspects of operation and wear of such coatings.

### 1.2. Literature review

Tabakov et al. [7, 8] considered mechanisms of cracking with respect to single-layer macroscale coatings on the basis of systems composed of TiN, TiCN, (Ti,Zr)N, and (Ti,Zr)CN. They discovered that coatings of a complex composition of (Ti,Zr)N and (Ti,Zr)CN are characterized by better resistance to intensive cracking. Tabakov et al. also considered multilayered coatings with macroscale structure: in particular, on the basis of systems composed of TiCN-(Ti,Zr)N-TiN, TiN-(Ti,Zr)N-TiN, TiCN-(Ti,Al)N-TiN, and TiCN-(Ti,Mo)N-TiN [9]. These studies proved that the introduction of zirconium nitride in the coating composition significantly reduces the tendency to cracking. The problems of cracking and brittle fracture of coatings consisting of Ti-TiN-(Ti,Cr,Al)N, Zr-(Zr,Cr)N-CrN, and Ti-TiN-(Ti,Cr,Al)N and Ti-(Al,Cr)N-(Ti,Al)N, Ti-(Al,Cr)N-(Ti,Cr,Al)N, and Zr-(Al,Cr)N-(Zr,Cr,Al)N also were addressed in papers [10–16]. A detailed review of existing papers in the field of crack formation in multilayered coatings, with classification of types of cracks and analysis of the mechanisms of their formation, is given in [17]. The topic of mathematical modeling of cracking in multilayered coatings with the use of an axis-symmetrical finite element method (FEM) model was considered by Skordaris et al. [18]. Wu et al. [19, 20] modeled cracking in single-layer coatings within the framework of linear elastic fracture mechanics (LEFM). M'Saoubi et al. [21] investigated the nature of wear, including brittle fracture

and cracking of physical vapor deposition (PVD)-coated (TiN, (Ti,Si)N, (Ti,Al)N, and (Al,Cr)N) polycrystalline cubic boron nitride. Koseki et al. [22] examined the cutting performance of TiN-coated cutting tools. Defects (e.g., droplets, voids) in the coating were found to be the starting point of damage. The breakdown region is enlarged as the work material is caught in the damaged portion of the coating. Kumar and Curtin [23] considered the probable mechanisms of development and inhibition of cracks in microstructures: particularly at crack bridging by ductile ligaments, crack deflection by second-phase particles, microcrack formation, and stress-induced phase transformations. The same paper also includes an overview of methods for modeling the development of cracks using FEM and incorporating cohesive elements at the continuum level, as well as discrete dislocation methodology at the mesoscopic level, and coupled atomistic/continuum methods that transition atomic level information to the microscopic level. A large number of studies have been devoted to the investigation of causes and conditions for the formation of delaminations in multilayered composite macrostructures. To predict the occurrence of delaminations, the methods of layer-wise interface elements [24, 25], classical finite element analysis (FEA) [25, 26], and the virtual crack closure technique (VCCT) [27] are widely used. The issues concerning delamination of multilayered nanostructured coatings are also discussed in details in [28].

### 1.3. Mechanisms of crack formation

Starting from the theory of crack formation [3–5], the concentration of local tensile stresses  $\sigma_{ld}$  in the head of a series of edge dislocations caused by the action of a number of edge stresses  $\tau$  can be determined using the following equation [29]:

$$\sigma_{ld} = \sqrt{\frac{d}{2x}}(\tau - \tau_i) \quad (1)$$

where  $2d$  is the length of the slip band or the distance between the slip bands (the value may also correspond to crystalline grain diameter),  $x$  is the distance from the strip to the head of the cluster of dislocations, and  $\tau_i$  is the stress of resistance to movement of dislocations (friction stress). If the local stress reaches the theoretical strength of the crystalline body  $\sigma_{theor}$  determined by the equation

$$\sigma_{theor} = \sqrt{\frac{E\gamma}{a_0}} \quad (2)$$

where  $a_0$  is the equilibrium distance between atoms,  $E$  is the modulus of elasticity, and  $\gamma$  is the plastic shear deformation, then conditions arise for the formation of a dislocation microcrack. Consequently, the criterion for the formation of a microcrack is as follows:

$$\sqrt{\frac{d}{2x}}(\tau - \tau_i) \geq \sqrt{\frac{E\gamma}{a_0}} \quad (3)$$

The number of positive or negative dislocations in a flat cluster near an obstacle can be expressed by an approximate formula (assuming  $E \approx 2G$ , where  $G$  is the shear modulus):

$$n \approx \frac{(\tau - \tau_i)}{bE} \quad (4)$$

Assuming the additional condition of  $x \approx a_0$ , from the joint solution of Eqs. (3) and (4), we obtain the condition necessary for the formation of a microcrack under the dislocation mechanism:

$$(\tau - \tau_i)nb = 2\gamma \quad (5)$$

Analysis of the given conditions for the formation of a dislocation microcrack results in the following conclusion. Local tensile stresses in the head of a number of dislocations are formed primarily because of tangential stresses  $\tau$  and are not related in any way to tensile stresses (i.e., only shear stresses are crucial for the initiation of a microcrack). The defects already existing or emerging in the early stages of deformation of solid bodies result in the initiation and development of the failure processes. Various mechanisms of failure are realized depending on the structural and stress strain states of a solid body and also depending on the external medium [3, 6, 30]. The following are the most common mechanisms of microfailure of metals (**Figure 1**):

1. Viscous fracture (**Figure 1a**). This mechanism of failure is caused by the formation of micropores near inclusions or particles of the second phase, their growth, localization of microplastic deformation in the crosspieces between the pores, and, in the final stage, the fusion of micropores and the break of the bridges. The model and criterion for the formation of micropores are as follows: a micropore is formed when the cohesive stresses (bond stresses between the inclusion particles and the matrix) reach a critical stress. The existing models for the formation, growth, and fusion of micropores can be used to analyze micromechanisms of viscous fracture of a solid body in front of a crack tip. When the stresses in front of the inclusions (before a crack tip) reach critical values, the micropores are being formed. Further growth of micropores and localization of plastic deformation results in plastic blunting of crack tip, merging of micropores with crack tip, and subsequent growth of a viscous crack (**Figure 2**). In multilayered composite nanostructured coatings, such a mechanism of cracking can occur primarily in the formation of delaminations at interlayer boundaries, as well as at the boundaries of nano-sublayers.
2. Transcrystallite cleavage (**Figure 1b**). This mechanism is characterized by failure of a solid body (spread of a crack) along certain crystallographic planes. In polycrystalline bodies, the process of transcrystallite cleavage is realized not in one crystallographic plane, but through the distribution and subsequent integration of a multitude of microcracks of the cleavage that arises in a certain family of crystallographic grain planes. As a rule, transcrystallite cleavage is of a brittle nature, although plastic deformation processes are also possible. The described mechanism can be typical for the formation of cracks in monolithic single-layer coatings (TiN, ZrN, etc.), as well as in monolithic layers of multilayered coatings. In coatings with nano-sublayers, the development of cracks under the above mechanism is significantly constrained by the boundaries of nano-sublayers.
3. Intercrystallite fracture (**Figure 1c**). This mechanism consists of the initiation and propagation of microcracks along grain boundaries. This failure mechanism is related to the fact that the fracture energy necessary for propagation of a crack along the grain boundaries is lower than the corresponding energy of the transcrystallite cleavage. In the coatings,

intergranular fracture can occur in monolithic single-layer coatings (in particular, transverse cracks in the columnar crystalline structure of TiN are formed under the above mechanism). As a rule, several mechanisms of failure take place simultaneously, and as a consequence, a mixed type of failure occurs. Typically, three types of loading or displacement of the points of crack surfaces under the influence of an external load are considered [3, 4, 6]. The first type (type 1) includes the formation of normal detachment cracks, characterized by movement of the points of the crack surface under the action of a load in the direction perpendicular to the plane of the crack. In this case, the crack tends to open. Cracks of the transverse type (type 2) are cracks in which points of surfaces are displaced across the front of the crack (leading edge of the crack). Finally, longitudinal shear cracks (type 3) are characterized by displacement of the points of the crack surface along its front. It should be noted that these types of loading can be combined, thus forming complex types of loading. The conditions of operation of multilayered nanostructured modified coatings for a metal-cutting tool are most typically characterized by loading of type 1 (typical for the rake face of the tool, due to the constant formation and failure of adhesion bridges with the tool being machined) and type 2 (typical for the flank face of the tool, due to longitudinal compressive stresses and the resulting plastic deformation of a substrate). To describe the delamination process, it is also possible to use strain energy release rate (SERR), which represents energy dissipated during fracture per unit of newly created fracture surface area [31]. Delamination growth rates were correlated with the SERR by means of the Paris relation [32, 33]:

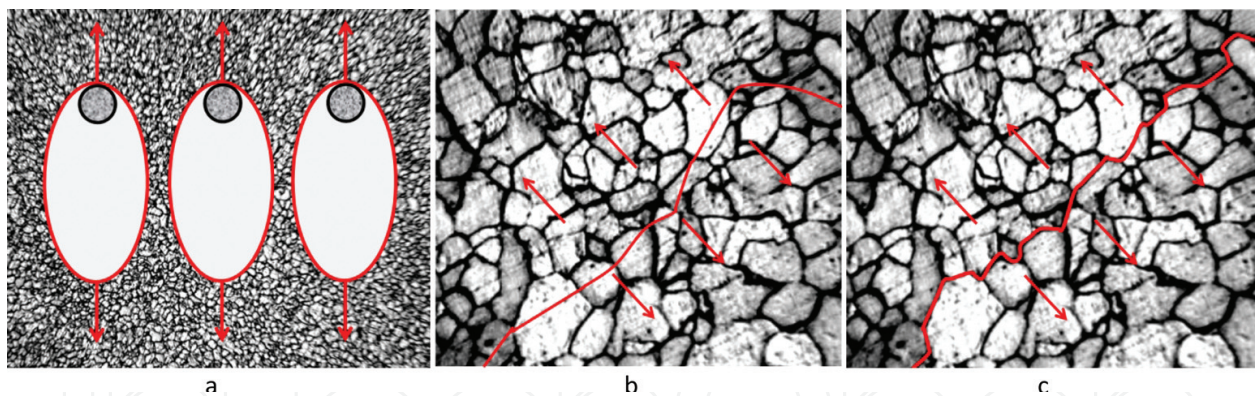


**Figure 1.** Mechanisms of failure: (a) viscous fracture, (b) transcrystallite cleavage, and (c) intercrystallite fracture.

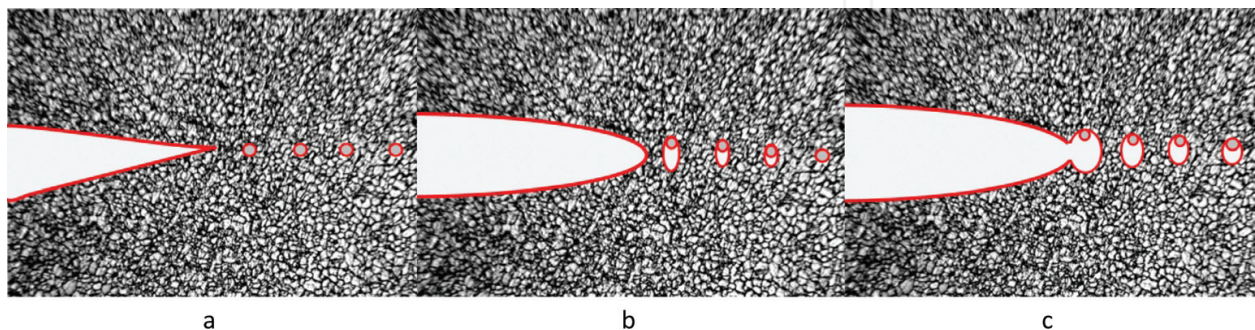


**Figure 2.** Pattern of the micromechanism of growth of a viscous crack: (a) inclusions at the crack tip, (b) growth of micropores in front of the crack tip, and (c) micropores merging with the crack tip.

$$\frac{dB_d}{dN} = Cf(G)^{n_p} \quad (6)$$

where  $B$  is delamination length (mm),  $N$  is the number of cycles,  $C$  is the Paris coefficient for delamination growth,  $G$  is the strain energy release rate (N/mm),  $n_p$  is the Paris exponent for delamination growth, and  $C$  and  $n$  are empirically determined parameters that depend on the materials and the temperature (and possibly other factors). As yet, no consensus has been reached on the correct form of  $f(G)$ . In particular,  $f(G)$  can be represented as SERR at maximum fatigue load,  $G_{max}$ , and within the SERR range,  $\Delta G$ . In turn,  $\Delta G$  can be determined from the following formula [25]:

$$\Delta G = \left( \sqrt{G_{max}} - \sqrt{G_{min}} \right)^2 \quad (7)$$

The dependence (1) also can be represented by [26] as follows:

$$\frac{dB_d}{dN} = C(G_{max})^{n_p} \quad (8)$$

where  $G_{max}$  is the strain energy release rate at maximum fatigue load (N/mm).

Thus, the task of the present work is to study the process of delamination between layers of multilayer coatings and between nano-sublayers of nanostructured coatings. These processes have a significant impact on the overall performance of modifying coatings and products with such coatings (in particular, metal-cutting tools). An important feature of this work is that not only laboratory samples but also cutting tool samples that underwent cutting tests in real production conditions were considered. The peculiarities of delamination were investigated depending both on the elemental composition of the coatings and on their architecture (total coating thickness and thickness of the nanolayers).

## 2. Materials and methods

### 2.1. Deposition method

For deposition of nanoscale multilayered composite coatings (NMCC), a vacuum-arc VIT-2 unit [2], which was designed for the synthesis of coatings on substrates of various tool materials, was used. The unit was equipped with an arc evaporator with filtration of vapor-ion flow. In this study, the process, termed filtered cathodic vacuum-arc deposition (FCVAD) [10–16], was used for deposition of coatings on the tools to significantly reduce the formation of the droplet phase during formation of the coating. The use of the FCVAD process does not cause structural changes in carbide and provides the following:

- High adhesive strength of the coating in relation to the carbide substrate.
- Control of the level of the “healing” of energy impact on surface defects in carbide in the form of microcracks and micropores and formation of favorable residual compressive stresses in the surface layers of the carbide material.

- Formation of the nanoscale structure of the deposited coating layers (grain size, sublayer thickness) with high density due to the energy supplied to the deposited condensate and transformation of the kinetic energy of the bombarding ions into thermal energy in local surface volumes of carbide material at an extremely high rate of approximately  $10^{14} \text{ K s}^{-1}$ .

When choosing the composition of NMCC layers, in forming the coating of the three-layered architecture [2, 10], the Hume-Rothery rule was used. This rule states that the difference in atomic dimensions in contacting compounds should not exceed 20% [34]. The parameters used at each stage of the deposition process of NMCC are shown in **Table 1**.

An uncoated carbide tool and a carbide tool with “reference” coating TiN, deposited via standard vacuum-arc technology of arc-PVD, were used as objects for comparative studies of tool life.

## 2.2. Microstructural studies

For microstructural studies of samples of carbide with coatings, a raster electron microscope FEI Quanta 600 FEG was used. The studies of chemical composition were conducted using the same raster electron microscope. To perform X-ray microanalysis, characteristic X-ray emissions resulting from electron bombardment of a sample were examined. The hardness (HV) of coatings was determined by measuring the indentation at low loads according to the method of Oliver and Pharr [35], which was conducted on a micro-indentometer microhardness tester (CSM Instruments) at a fixed load of 300 mN. The penetration depth of the indenter was monitored so that it did not exceed 10–20% of the coating thickness to limit the influence of the substrate. The adhesion characteristics were studied on a Nanovea scratch tester, which represents a diamond cone with apex angle of  $120^\circ$  and radius of top curvature of  $100 \mu\text{m}$ . The tests were conducted with the load linearly increasing from 0.05 to 40 N. Crack length was 5 mm. Each sample was subjected to three trials. The obtained curves were used to determine two parameters: the first critical load,  $L_{C1}$ , at which the first cracks appeared in the coating, and the second critical load,  $L_{C2}$ , which caused the total failure of the coating.

## 2.3. Study of cutting properties

A study of the cutting properties of the tool made of carbide with developed NMCC was conducted using a lathe CU 500 MRD for longitudinal turning of steel C45 (HB 200). In the experiment, the cutters featured mechanical fastening of inserts made of carbide (WC + 15%

Process	$p_N$ (Pa)	$U$ (V)	$I_{Al}$ (A)	$I_{ZrNb}$ (A)	$I_{Ti}$ (A)	$I_{Cr}$ (A)
Pumping and heating of vacuum chamber	0.06	+20	120	80	65	75
Heating and cleaning of products with gaseous plasma	2.0	100 DC/900 AC f = 10 kHz, 2:1	80	—	—	—
Deposition of coating	0.36	–800 DC	160	75	55	70
Cooling of products	0.06	—	—	—	—	—

Note:  $I_{Ti}$  = current of titanium cathode,  $I_{Al}$  = current of aluminum cathode,  $I_{ZrNb}$  = current of zirconium-niobium cathode,  $I_{Cr}$  = current of chromium cathode,  $p_N$  = gas pressure in chamber, and  $U$  = voltage on substrate.

**Table 1.** Parameters of stages of the technological process of deposition of NMCC.

TiC + 6% Co) with square shapes (SNUN ISO 1832:2012) and with the following figures for the geometric parameters of the cutting part:  $\gamma = -8^\circ$ ,  $\alpha = 6^\circ$ ,  $K = 45^\circ$ ,  $\lambda = 0$ , and  $R = 0.8$  mm. The study was performed for the following cutting modes:  $f = 0.2$  mm/rev,  $ap = 1.0$  mm, and  $vc = 250$  m  $\text{min}^{-1}$ . Flank wear-land values ( $VB_c$ ) were measured with a toolmaker's microscope MBS-10 as the arithmetic mean of four to five tests. A value of  $VB_c = 0.4$  mm was taken as failure criterion. The study included statistical processing of tests of wear of cutting tools, sample mean value of wear, and sample mean square deviation of tool wear, which are random variables with different values in repeated experiments. Of note, during the experiments, outlying results were excluded. To exclude outlying results of the experiments, Irwin's criterion was used. To do that, the value of Irwin's criterion  $K_\lambda$  was defined, if the outlying result was the maximum value  $VB_{max}$ :

$$K_\lambda = (VB_c - VB_{max})/K_\sigma \quad (9)$$

and if the doubts were provoked by the wear value with minimum value  $VB_{min}$ :

$$K = (VB_c - VB_{min})/K_\sigma \quad (10)$$

The calculated value  $K_\lambda$  was compared to the critical value  $K_{\lambda A}$ , defined theoretically for a given level of significance level  $A$  and selection criterion  $n$ . If  $K_\lambda < K_{\lambda A}$ , then deviation of questionable value  $VB_c$  was considered as valid.

### 3. Results and discussion

#### 3.1. Adhesion characteristics

The classical test that enables determination of the strength of the adhesive bond of a coating with a substrate by the scratch-test method also can be used for qualitative evaluation of the strength of the adhesive bond between individual coating layers and cohesive bond between nano-sublayers. The tests were conducted on a Nanovea scratch tester. The indenter was a diamond cone with an apex angle of  $120^\circ$  and radius of top curvature of  $100 \mu\text{m}$ . The tests were performed with a load linearly increasing from  $0.05$  N to the final load ( $40$  N). Crack length was  $5$  mm. Each sample was subjected to three trials. The obtained curves were used to determine two parameters: the first critical load  $L_{C1}$ , at which first cracks appeared in NMCC, and the second critical load  $L_{C2}$ , which caused the total failure of NMCC. Typical types of failure are presented in **Figure 3** (standard coating TiN), **Figure 4** (NMCC Zr-ZrN-(Nb,Zr,Ti,Al)N), and **Figure 6** (NMCC Ti-TiN-(Ti,Al)N). All investigated coatings showed a sufficiently high level of adhesion bonds with substrate. Numerous research efforts and the experience of the authors of this paper show that a scratch test does not have a unique correlation with the tool life of a coated tool [1]; the test allows only "rejecting" coatings with insufficient strength of adhesion bonds. However, this test enables a study of the nature of the coating failure, particularly from the point of view of delaminations that occur in its structure. Let us consider the nature of the failure of the single-layer monolithic TiN coating (**Figure 3**). A fairly smooth scribing groove is clear, with a clearly visible area of brittle fracture of the outer area of the coating. On the edges of the groove, cracks and splintered areas of the coating are visible. Patterns of failure of

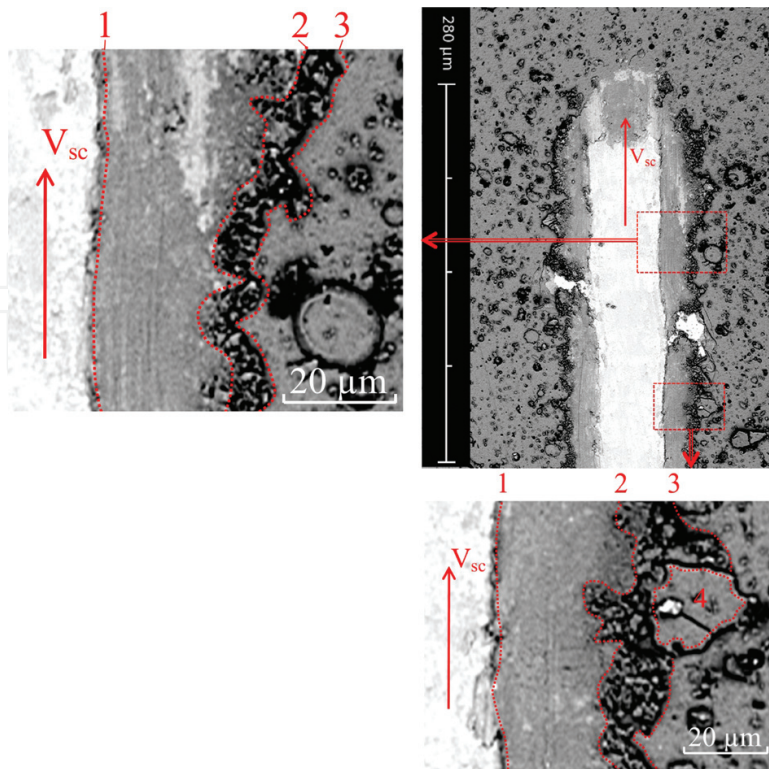


**Figure 3.** The nature of failure of coating TiN along a longitudinal crack, caused by a diamond indenter at critical (breaking) load [28].  $V_{sc}$ , scribing direction. (1) “Substrate-coating” boundary, (2) boundary of the brittle fracture zone of the coating, (3) boundary of the scribing groove, and (4) splintered section of the coating.

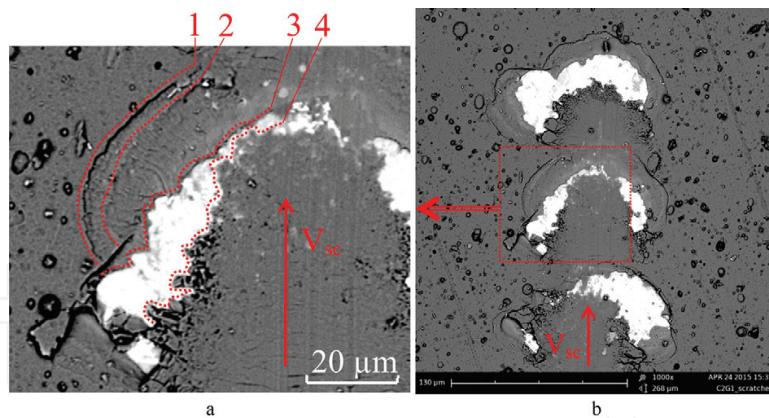


**Figure 4.** The nature of failure of NMCC Zr-ZrN-(Nb,Zr,Ti,Al)N along a longitudinal crack, caused by a diamond indenter at critical (breaking) load.  $V_{sc}$ , scribing direction [28]. (1) The boundary of the wedging spallation zone, (2) the delamination boundary between the intermediate and wear-resistant layers, (3) the boundary of “adhesion coating layer-substrate” delamination, and (4) the boundary of the coating zone, pressed by the tip of the scratch tester.

NMCC Zr-ZrN-(Nb,Zr,Ti,Al)N (**Figure 4**) and (NMCC Ti-TiN-(Ti,Al)N) (**Figure 5**) are characterized by a number of significant differences. The failures of those coatings occur under the mechanism of “wedging spallation.” Meanwhile, NMCC Zr-ZrN-(Nb,Zr,Ti,Al)N shows extensive interlayer delaminations, whereas in NMCC Ti-TiN-(Ti,Al)N, similar delaminations are less pronounced, and delaminations between nano-sublayers also occur. Generally, this picture correlates with the nature of the failure of those coatings observed during cutting tests.

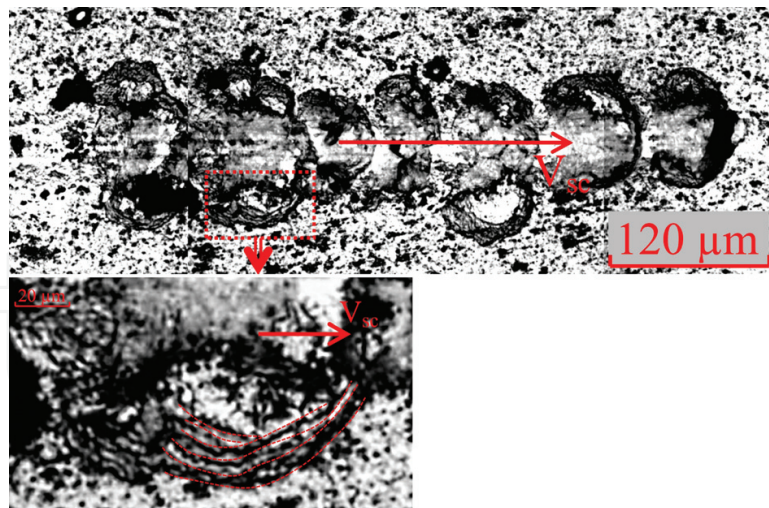


**Figure 5.** The nature of failure of NMCC Ti-TiN-(Ti,Al)N along a longitudinal crack, caused by a diamond indenter at critical (breaking) load [28].  $V_{sc}$ , scribing direction.

The study of the scribing process for nanostructured coatings of large thickness (exceeding  $10\ \mu\text{m}$ ) is of particular interest. In this case, it is possible to observe both coating failure caused by violation of adhesion bonds between layers and cohesive bonds between nano-sublayers and failure of a coating as a whole, when failure is not accompanied by delamination. Signs of failure of coating Ti-TiN-(Ti,Al)N (with coating thickness  $13\ \mu\text{m}$ ) at scribing are shown in **Figures 6** and **7**.

In particular, **Figure 6** shows both violation of the interlayer interface between layers TiN and (Ti,Al)N and persistence of strong adhesion bonds between nano-sublayers of layer (Ti,Al)N. At zoom in, it is possible to notice in **Figure 7** that in some cases, at critical loads, there is also failure of cohesive bonds between nano-sublayers, and that fact results in formation of a kind of “terraces,” i.e., flat microsities with surface structure of a nano-sublayer. It is also possible to see signs of a tear-out of microdroplets embedded in the coating structure. **Figure 7** shows the “terrace-like” structure of failure zone of a nanostructured coating. A general structure of the coating under the study and the nature of cracking in it during the cutting tests are shown below, in **Figure 20**.

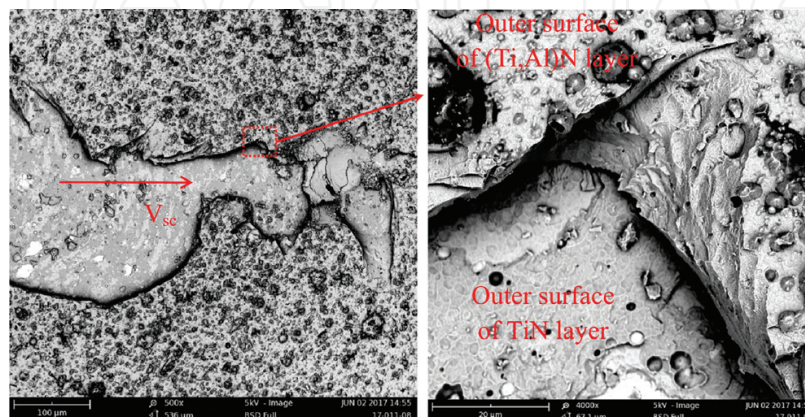


**Figure 6.** The nature of failure of NMCC Ti-TiN-(Ti,Al)N (coating thickness  $13\ \mu\text{m}$ ) along a longitudinal crack, caused by a diamond indenter at critical (breaking) load [28].

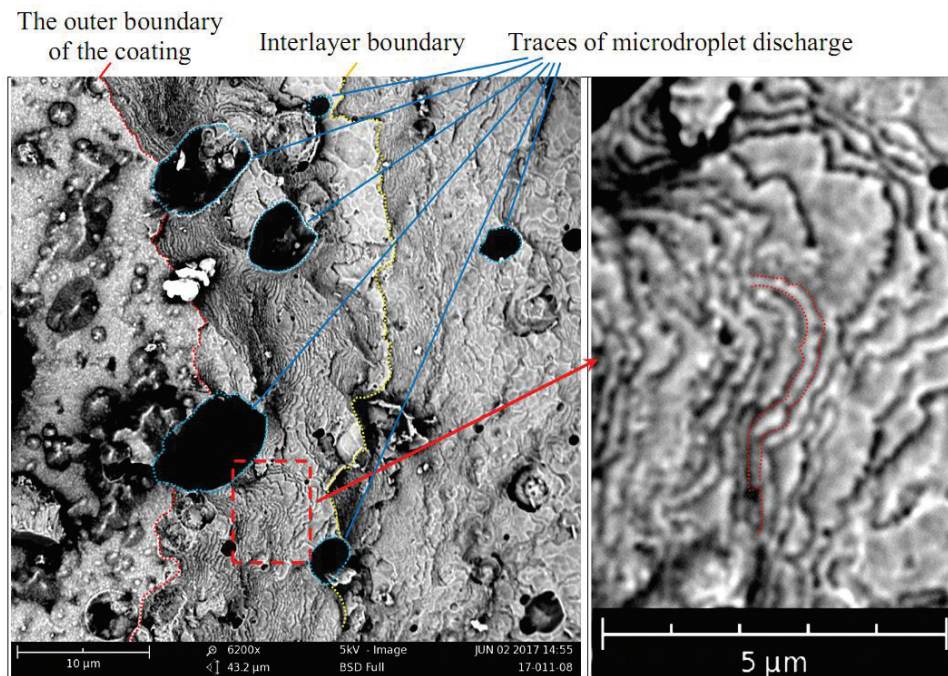


**Figure 7.** The nature of failure of NMCC Ti-TiN-(Ti,Al)N (coating thickness 13  $\mu\text{m}$ ) along a longitudinal crack, caused by a diamond indenter at critical (breaking) load [28].

### 3.2. Determination of basic properties of NMCC under cutting tests

This study was focused on the NMCC containing nitrides of Ti, Al, Cr, Zr, and Nb in its composition. For the detailed studies of various properties, NMCC were selected based on the following conditions:

- If earlier studies show significant increase in cutting properties and reliability of the tool [10–16].
- If the thermodynamic criterion  $\Delta rG$  (Gibbs free energy change per mole of reaction) favored the formation of the NMCC.

To accomplish the research tasks, NMCC of various compositions were selected to meet the above conditions and were deposited using the FCVAD technology. The thicknesses of the coatings used in the studies were 2.4–5.0  $\mu\text{m}$ . A wide range of thicknesses were selected on the basis of previous studies (in particular [10–16]), indicating the improvement in cutting performance with increase in coating thickness. The basic properties of the NMCC under study are presented in **Table 2**. Curves obtained by mathematical processing of the experimental data are shown in **Figure 8**.

The NMCC Ti-TiN-(Ti,Al)N shows better resistance for approximately 19 min of operation due to its high surface hardness; however, subsequently, the tool with such a coating begins to experience intensive wear. This fact can be related to the start of intense cracking and wear of this coating. As a result, the tool with NMCC Zr-ZrN-(Zr,Cr,Al)N showed better resistance, and it was characterized by a balanced combination of sufficiently high hardness and resistance to brittle fracture. Let us consider in detail the mechanism of cracking and failure of coatings, paying special attention to such aspects of those processes as longitudinal cracks and

#	Composition of NMCC	Tool life $T_c$ (min) VB = 0.4 mm	Sublayer thickness (nm)	Total thickness ( $\mu\text{m}$ )	Adhesion, $L_{C2}$ (N)	Hardness, HV (GPa)
1	Uncoated	8	—	—	—	18
2	TiN	18	—	2.8	31	30
3	Zr-ZrN-(Zr,Cr,Al, Nb)N	24	200	3.8	>40	34
4	Zr-ZrN-(Nb,Zr,Ti, Al)N	31	45–60	3.3	>40	34
5	Ti-TiN-(Ti,Al)N	28	65–90	5.0	>40	38
6	Zr-ZrN-(Zr,Cr,Al)N	37	15–45	3.4	39	36

**Table 2.** The basic properties of NMCC and periods of tool life of the carbide tools under study with the NMCC under study.

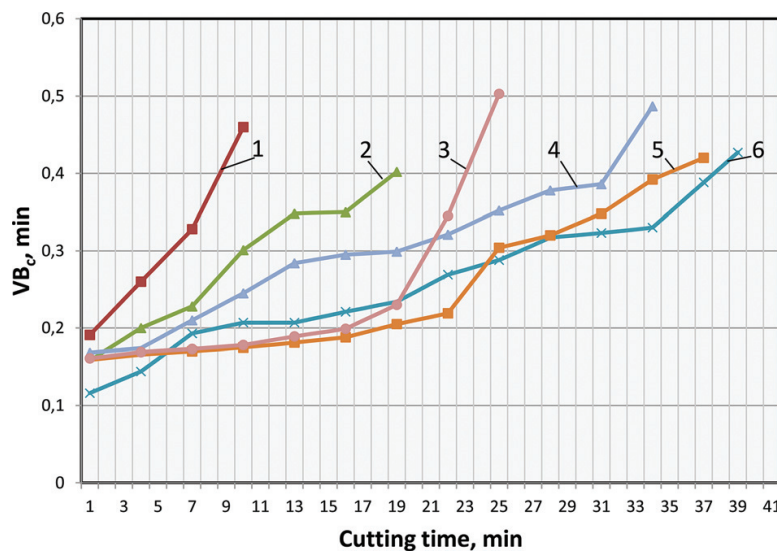


**Figure 8.** Dependence of wear VB on cutting time for dry turning of steel C45 at  $a_p = 1.0$  mm,  $f = 0.2$  mm/rev, and  $v_c = 250$  m/min. (1) Uncoated, (2) TiN, (3) Zr-ZrN-(Zr,Cr,Al,Nb)N, (4) NMCC Zr-ZrN-(Zr,Cr,Al)N, (5) NMCC Ti-TiN-(Ti,Al)N, and (6) Zr-ZrN-(Zr,Cr,Al)N.

delaminations (interlayer delaminations and delaminations between nano-sublayers) form. Basic mechanism for the formation of longitudinal cracks and delaminations can be distinguished in a nanostructured multilayered coating because of the tearing force related to the adhesion interaction between the outer boundary of the coating and the material being machined (**Figure 9**), which has a prevailing fatigue characteristic and results in the formation of fatigue cracks due to the alternating processes of formation and failure of adhesion bridges in the system of “coating-material being machined.” The considered mechanism is more typical for coatings on the rake face of the tool.

The action of the mechanism shown in **Figure 9** can result not only in the formation of longitudinal cracks and delaminations but also in the destruction of the surface layers of the coating and, consequently, in the deterioration of the tool life of the metal-cutting tool (**Figure 10**).

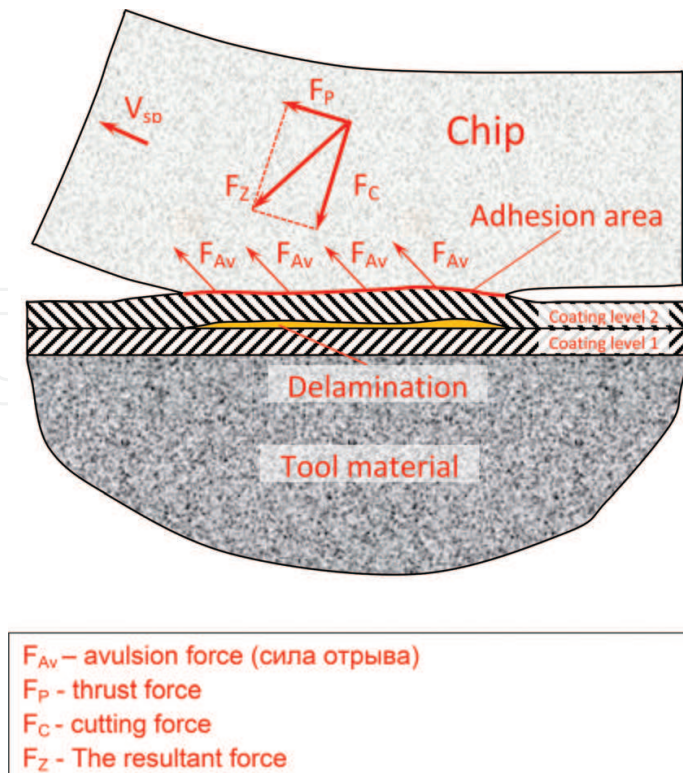


**Figure 9.** The mechanism of formation of longitudinal cracks and delaminations in a nanostructured multilayered coating during cutting due to the tearing force associated with adhesion interaction between the outer boundary of the coating and the material being machined [28].

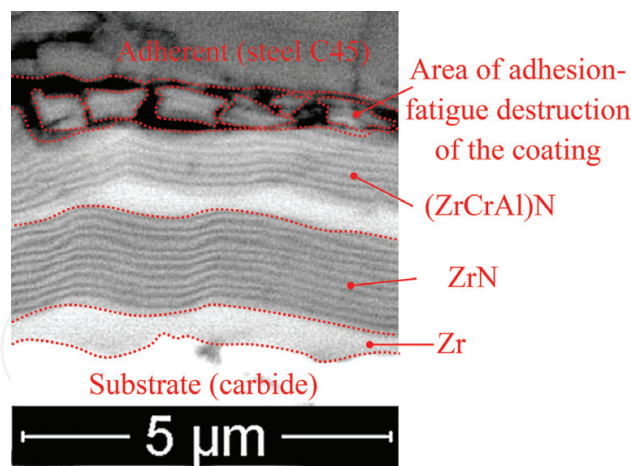


**Figure 10.** An example of the failure of the upper layer of NMCC Zr-ZrN-(Zr,Cr,Al)N because of the tearing force related to the adhesion interaction between the outer boundary of the coating and the material being machined (steel C45) [28].

An important distinctive feature of the development of longitudinal cracks in nanostructured coatings is the formation of bridges in the process of cracking due to the alternation of less plastic sublayers with more plastic ones in the coating structure. Such bridges inhibit the development of a crack by exerting a positive influence on coating crack resistance and, consequently, on the tool life of a cutting tool (**Figure 11**). This mechanism of inhibition of

cracking is fairly close to the mechanism of action of bridges from a particle of a more plastic phase embedded in the brittle phase described, in particular, by Kumar and Curtin [23]. It should be noted that the studies of the propagation of longitudinal cracks in monolithic coatings revealed no such bridges. The strength of the bridges depends on the composition of the coating layers. In particular, in layers of (Zr,Cr,Al)N (**Figure 11a**), the bridges show significantly higher strength and ductility than in (Zr,Nb,Ti,Al)N (**Figure 11b**), where the bridges show a tendency to failure.

No such bridges are observed in NMCC Ti-TiN-(Ti,Al)N, and that may be connected with the high hardness and brittleness of the layer (Ti,Al)N. The failure of NMCC Ti-TiN-(Ti,Al)N often occurs in accordance with a pronounced “brittle fracture” scenario with the formation of a network of longitudinal and transverse cracks (**Figure 12**).

In the case of insufficiently strong adhesion bond between the coating layers or cohesive bonds between its nano-sublayers, delaminations of the classical form are formed between the layers of the coating or between its nano-sublayers. In particular, **Figures 13** and **14** show obvious delamination between the intermediate TiN layer and the wear-resistant (Ti,Al)N layer. In the structure of the coating presented in **Figure 14**, transverse cracks and delaminations also occur between nano-sublayers of the wear-resistant layer. In addition, it is possible to note a relatively positive role of delamination (1) as a factor of inhibition of transverse cracks (3). The transverse cracks (3) are decelerated at the boundary of the intermediate and wear-resistant layers, and they are not spreading in the intermediate TiN layer (**Figure 14**).

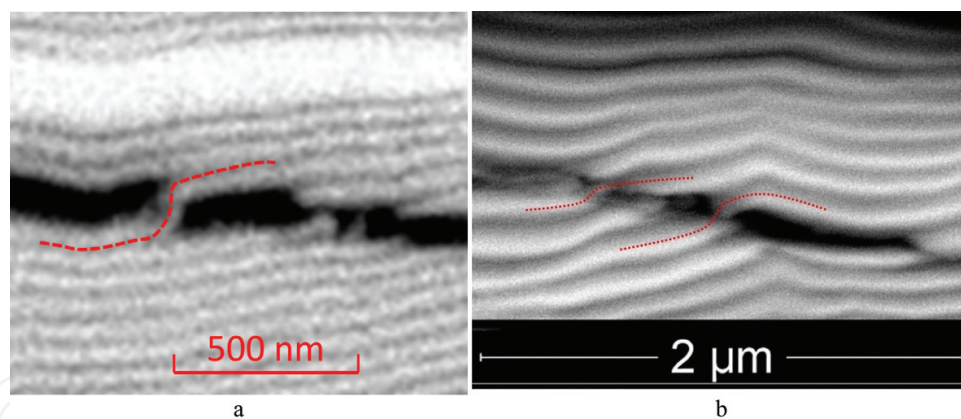


**Figure 11.** Deceleration of a longitudinal crack in NMCC Zr-ZrN-(Zr,Cr,Al)N (a) and Zr-ZrN-(Zr,Nb,Ti,Al)N (b) due the formation of bridges of more plastic nanolayers [17, 28].

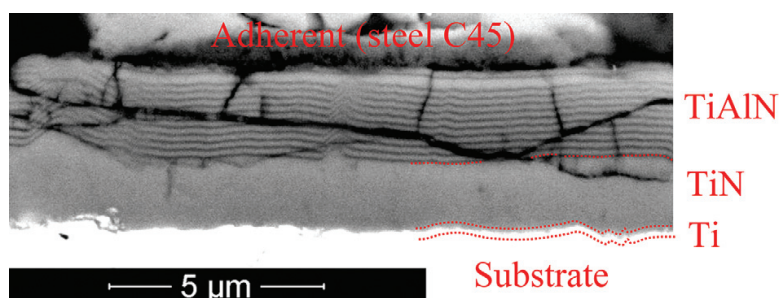


**Figure 12.** Failure of NMCC Ti-TiN-(Ti,Al)N with the formation of a network of longitudinal and transverse cracks [28].

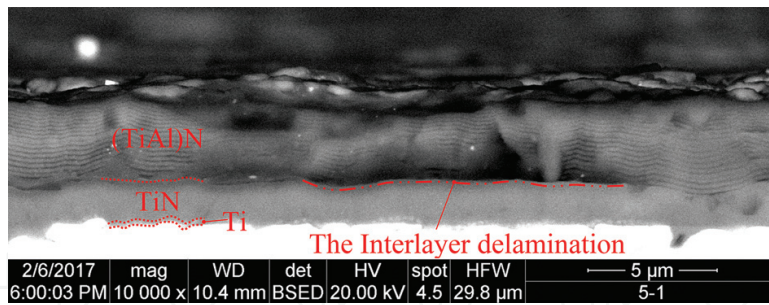


Figure 13. Interlayer delamination in the structure of NMCC Ti-TiN-(Ti,Al)N [28].

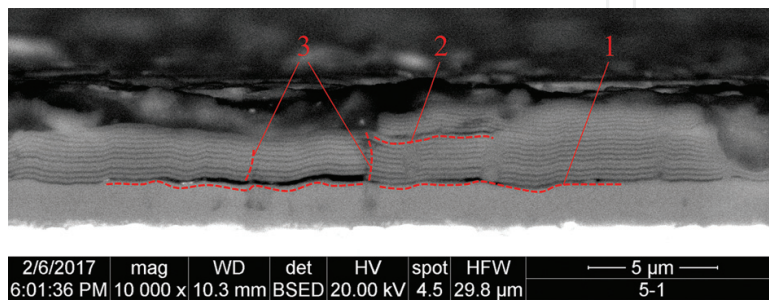


Figure 14. Interlayer delamination (1), delamination between nano-sublayers (2), and transverse cracks (3) in the structure of NMCC Ti-TiN-(Ti,Al)N [28].

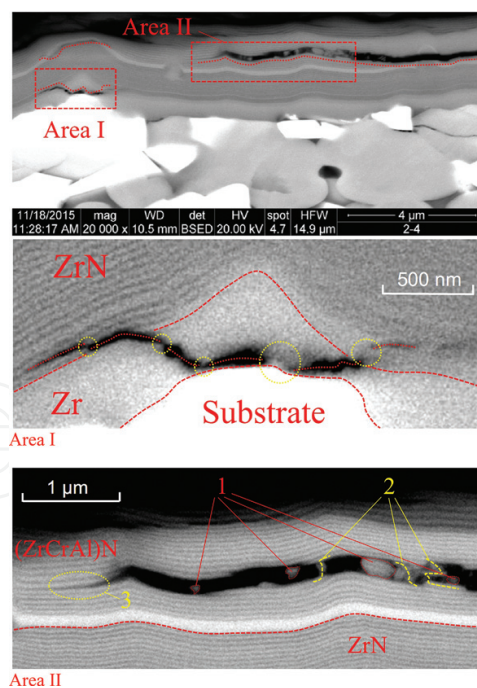


Figure 15. An example of formation of longitudinal cracks and delaminations in NMCC Zr-ZrN-(Zr,Cr,Al)N [28].

The patterns of formation of longitudinal cracks and delaminations often appear to be complex. In particular, **Figure 15** shows the mechanisms of cracking and delamination in NMCC Zr-ZrN-(Zr,Cr,Al)N. The area of this picture that is marked as AREA I contains a crack of a complex kind, combining delamination between the substrate and the adhesion layer Zr,

passing into a transverse crack that cuts the adhesive layer, and turning into a series of delaminations between nano-sublayers of the intermediate coating layer. The initial factor stimulating the formation of this crack is microroughness of the substrate, formed by high carbide grain. In contrast, the area indicated as AREA II contains an example of extended delamination, reaching a width of 200–300 nm. The formation of this delamination resulted in (1) chipping of microcomponents of the coating, (2) formation of bridges of more plastic nanolayers, and (3) the crack development boundary.

Various defects in coatings (in particular, embedded microdroplets and pores) can play an important role in the formation of longitudinal cracks and delamination. **Figure 16** shows how a crack reaches a macro droplet and forms branches. Meanwhile, one of the branches of the crack passes through a macro droplet, while the second crack branch traverses it along the contour. This photomicrograph reveals a separation of the material being machined from the coating; this separation indicates a low adhesive bond between the materials. Meanwhile, no separation of the coating from the tool material occurs due to a strong adhesive bond between them.

Another example of the effect of a microdroplet embedded in the structure of the coating on the formation of delaminations is shown in **Figure 17**. Here, a crack is formed directly above a microdroplet, and several parallel delaminations exist in the area adjacent to a microdroplet. These occurrences may be related to internal stresses arising during the coating deposition.

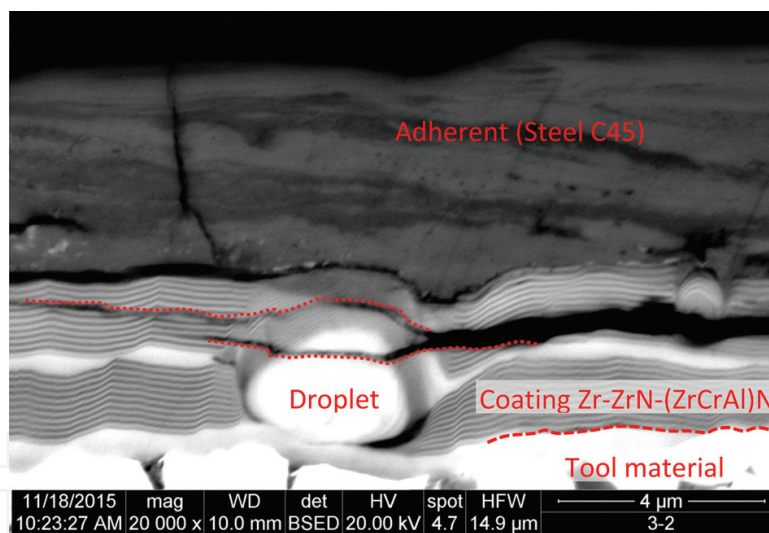


**Figure 16.** An example of development of a longitudinal crack in NMCC Zr-ZrN-(Zr,Cr,Al)N [28].

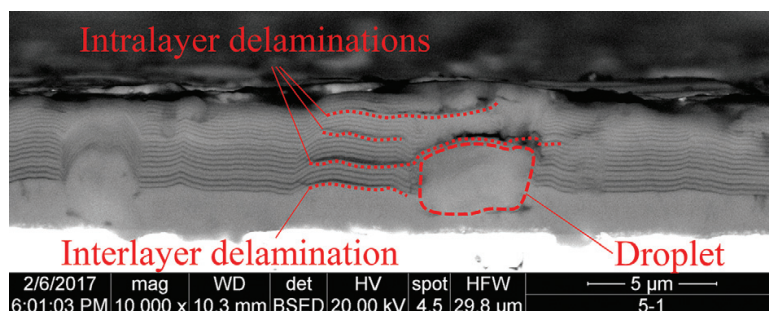


**Figure 17.** An example of development of a longitudinal crack in NMCC Ti-TiN-(Ti,Al)N [28].

Let us consider separately the process of delamination and failure in coating Zr-ZrN-(Zr, Cr, Al, Nb)N with thickness of sublayers of about 200 nm (**Figure 18a**). Due to thick sublayers, this coating cannot be called “nanostructured.” This coating is characterized by a large number of delaminations, arising especially in the fracture zone adjacent to a wear crater. No bond bridges are formed between sublayers (**Figure 18 Area A**), while delaminations are an important factor in failure of coating (**Figure 18c**).

Let us individually consider delaminations formed in NMCC of heavy thickness (usually exceeding 8  $\mu\text{m}$ ) because of heavy internal compressive stresses. Such delaminations can be formed with equal probability in the coating both on the rake and flank face of a tool. An example of formation of delaminations in “thick” NMCC is presented in **Figure 20**. It is possible to observe four clear delaminations located at approximately equal distance (about 20 nano-sublayers) from each other. Meanwhile, the delamination closest to the substrate (area A on **Figure 20**) passes exclusively along the boundary between the sublayers. At the same time, delaminations B, C, and D are rather longitudinal cracks because they also are characterized by breaks in the structures of nano-sublayers (**Figure 19**).

Various internal defects in “thick” NMCC (in particular, microdroplets embedded in the structure of the coating) become particularly important and result in local fracture of the coating because of the formation of multiple delaminations that weaken the coating structure and ultimately result in the formation of a transverse crack (**Figure 20**). As a result of the distortion of the coating structure associated with the curvature of the nano-sublayers because of rounding

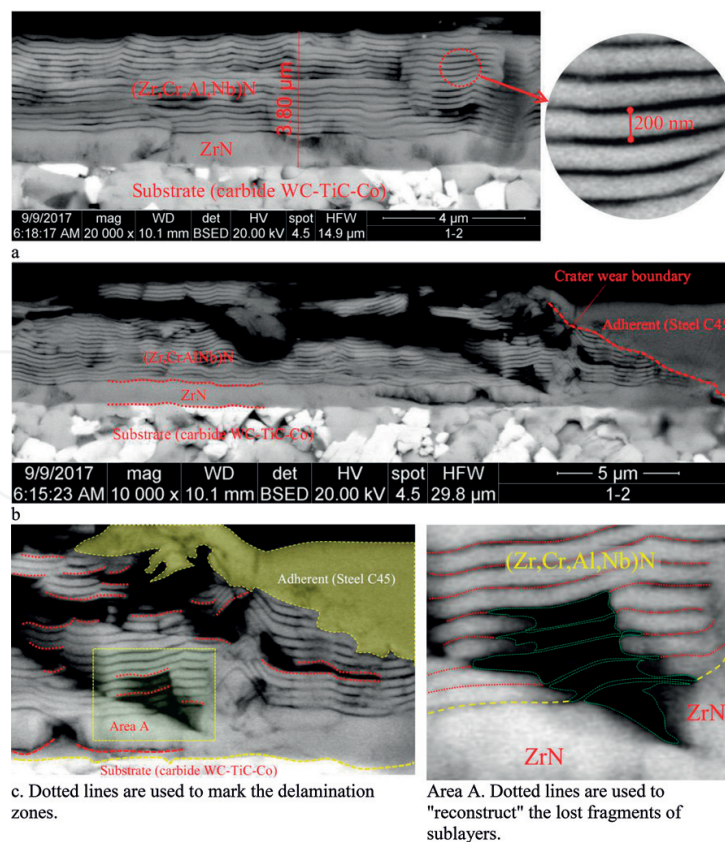


**Figure 18.** The process of delamination and failure in coating Zr-ZrN-(Zr,Cr,Al,Nb)N: general structure (a), destruction of the coating in the area of the crater wear boundary (b), boundary region “coating-adherent” (c).

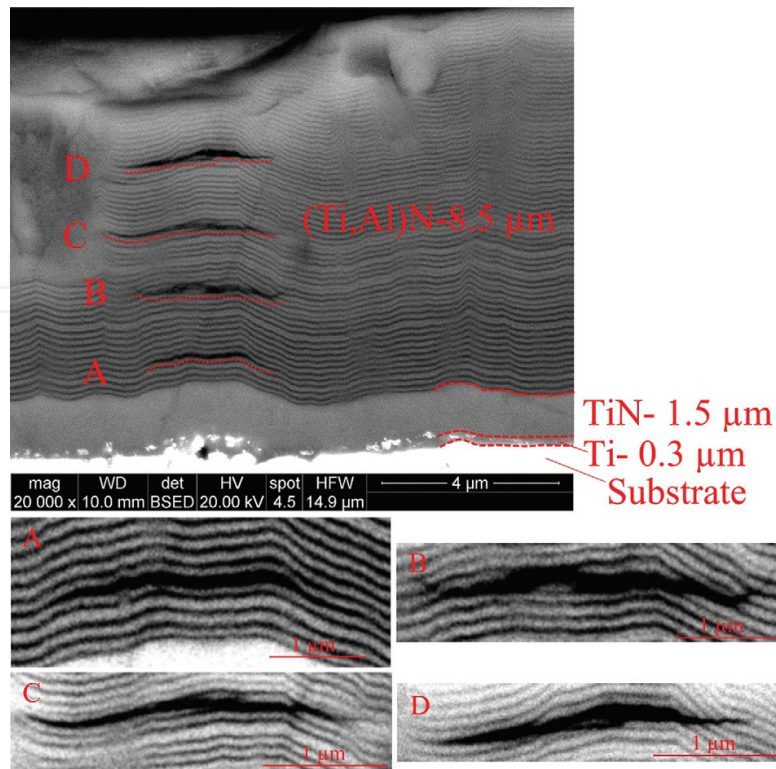


**Figure 19.** An example of the formation of delaminations in NMCC Ti-TiN-(Ti,Al)N (total thickness of the coating is 10.3 μm) [28].

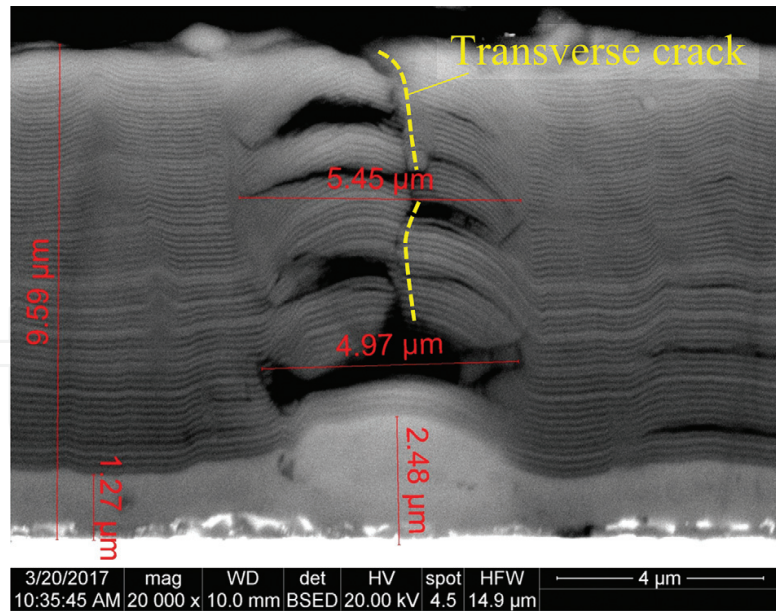


**Figure 20.** Formation of a transverse crack in the structure of NMCC Ti-TiN-(Ti,Al)N as a result of weakening of the structure of NMCC by multiple delaminations formed under the influence of internal stresses [28].

of an embedded microdroplet, internal stresses arise, which in turn result in the formation of corresponding delaminations and longitudinal cracks. Because (Ti,Al)N is a very hard, yet brittle compound, the chipping of fragments of nano-sublayers and formation of a transverse crack occur in the coating structure weakened by delaminations.

## 4. Conclusions

This study of the nature of the formation of longitudinal cracks and delaminations in multi-layered nanostructured coatings reveals the following:

1. Two important mechanisms result in formation of transverse cracks and delaminations:
  - a. Tearing force associated with adhesion interaction between the outer boundary of the coating and the material being machined (typical for the rake face of the tool).
  - b. Tearing force associated with plastic microdeformations in the surface layer of the tool substrate (more typical for the flank face of a tool).
2. The nature of the formation of longitudinal cracks and delaminations varies significantly for different coating compositions. In coatings with more plastic nanolayers, bridges can be formed, which inhibit the development of cracks. This can be clearly observed in NMCC Zr-ZrN-(Zr,Cr,Al)N and to a lesser extent in NMCC Zr-ZrN-(Zr,Nb,Ti,Al)N, while in coatings with more hard and brittle nanolayers (e.g., (Ti,Al)N), such bridges are not formed, and coatings are destructed under the mechanism of brittle failure.
3. Such coating defects as embedded microdrops and micropores can stimulate the development of longitudinal cracks and delaminations.
4. The following factors reduce the probability of formation of longitudinal cracks (delamination):
  - a. Reduction of adhesion interaction between the outer boundary of the coating and the material being machined.
  - b. Increase of adhesion bonds between coating layers and cohesive bonds between the nano-sublayers.
  - c. Decrease in the level of plastic microdeformations of the tool substrate, in particular, through heat strengthening and/or diffusion saturation with alloying elements.
5. In general, coatings with thickness of sublayers of more than 100 nm do not form bond bridges which inhibit cracking. In such coatings, delamination develops more actively and leads to failure of coating structure.
6. NMCC of relatively large thickness (larger than 8  $\mu\text{m}$ ) may experience delamination during the deposition as a result of significant internal stresses. The presence of such delamination can contribute to brittle fracture of coatings, particularly NMCC based on a hard and brittle compound (Ti,Al)N.

## Acknowledgements

This research was financed by the Ministry of Education and Science of the Russian Federation in the framework of the state order in the sphere of scientific activity (Leading researchers, project 16.9575.2017/6.7).

## Author details

Alexey Vereschaka<sup>1\*</sup>, Sergey Grigoriev<sup>1</sup>, Nikolay Sitnikov<sup>2</sup>, Gaik Oganyan<sup>1</sup>, Anatoliy Aksenenko<sup>1</sup> and Andre Batako<sup>3</sup>

\*Address all correspondence to: ecotech@rambler.ru

1 Moscow State Technological University STANKIN, Moscow, Russia

2 National Research Nuclear University MEPhI, Moscow, Russia

3 Liverpool John Moores University (LJMU), Liverpool, UK

## References

- [1] Vereschaka AS. Working Capacity of the Cutting Tool with Wear Resistant Coatings. Moscow: Mashinostroenie; 1993 (in Russian)
- [2] Vereshchaka AA, Vereshchaka AS, Mgaloblishvili O, Morgan MN, Batako Nano-scale AD. Multilayered-composite coatings for the cutting tools. *International Journal of Advanced Manufacturing Technology*. 2014;**72**(1):303-317. DOI: 10.1007/s00170-014-5673-2
- [3] Matvienko YG. The Models and Criteria of Fracture Mechanics. Moscow: FIZMATLIT; 2006 (in Russian)
- [4] Broberg KB. Cracks and Fracture. San Diego: Academic Press; 1999
- [5] Zehnder TA. Lecture Notes on Fracture Mechanics. Ithaca, New York: Cornell University; 2007
- [6] Anderson TL. Fracture Mechanics: Fundamentals and Applications. New York: CRC Press LLC; 1995
- [7] Tabakov VP. The influence of machining condition forming multilayer coatings for cutting tools. *Key Engineering Materials*. 2012;**496**:80-85
- [8] Tabakov VP, Vereschaka AS. Development of technological means for formation of multilayer composite coatings, providing increased wear resistance of carbide tools, for different machining condition. *Key Engineering Materials*. 2014;**581**:55-61
- [9] Tabakov VP, Smirnov MY, Tsirkin AV. Productivity of End Mills with Multilayer Wear-resistant Coatings. UISTU: Ulyanovsk; 2005 (in Russian)
- [10] Vereschaka AA, Vereschaka AS, Bublikov JI, Aksenenko AY, Sitnikov NN. Study of properties of nanostructured multilayer composite coatings of Ti-TiN-(TiCrAl)N and Zr-ZrN-(ZrNbCrAl)N. *Journal of Nano Research*. 2016;**40**:90-98. DOI: 10.4028/www.scientific.net/JNanoR.40.90
- [11] Vereschaka AA, Vereschaka AS, Batako AD, Hojaev OK, Mokritskii Y. Development and research of nanostructured multilayer composite coatings for tungsten-free carbides with extended area of technological applications. *International Journal of Advanced Manufacturing Technology*. 2016;**87**:3449-3457. DOI: 10.1007/s00170-016-8739-5

- [12] Volkhonskii AO, Vereshchaka AA, Blinkov IV, Vereshchaka AS, Batako AD. Filtered cathodic vacuum arc deposition of nano-layered composite coatings for machining hard-to-cut materials. *International Journal of Advanced Manufacturing Technology*. 2016;**84**:1647-1660. DOI: 10.1007/s00170-015-7821-8
- [13] Alexey AV, Sergey NG, Anatoly SV, Alexey YP, Batako AD. Nano-scale multilayered composite coatings for cutting tools operating under heavy cutting conditions. *Procedia CIRP*. 2014;**14**:239-244. DOI: 10.1016/j.procir.2014.03.070
- [14] Vereschaka AA, Volosova MA, Batako AD, Vereshchaka AS, Mokritskii BY. Development of wear-resistant coatings compounds for high-speed steel tool using a combined cathodic vacuum arc deposition. *International Journal of Advanced Manufacturing Technology*. 2016;**84**:1471-1482. DOI: 10.1007/s00170-015-7808-5
- [15] Grigoriev SN, Vereshchaka AA. Methodology of formation of multi-layered coatings for carbide cutting tools. *Mechanics & Industry*. 2016;**17**:706. DOI: 10.1051/meca/2016065
- [16] Vereschaka AA, Vereschaka AS, Batako ADL, Mokritskii BJ, Aksenenko AY, Sitnikov NN. Improvement of structure and quality of nano-scale multi-layered composite coatings, deposited by filtered cathodic vacuum arc deposition method. *Nanomaterials and Nanotechnology*. 2016;**7**:1-13. DOI: 10.1177/1847980416680805
- [17] Vereschaka AA, Grigoriev SN. Study of cracking mechanisms in multi-layered composite nano-structured coatings. *Wear*. 2017;**378-379**:43-57. DOI: 10.1016/j.wear.2017.01.101
- [18] Skordaris G, Bouzakis K-D, Charalampous P. A dynamic FEM simulation of the nano-impact test on mono- or multi-layered PVD coatings considering their graded strength properties determined by experimental-analytical procedures. *Surface & Coatings Technology*. 2015;**265**:53-61
- [19] Wu X-F, Dzenis YA, Strabala KW. Free-edge stresses and progressive cracking in surface coatings of circular torsion bars. *International Journal of Solids and Structures*. 2008;**45**:2251-2264
- [20] Wu X-F, Jenson RA, Zhao Y. Stress-function variational approach to the interfacial stresses and progressive cracking in surface coatings. *Mechanics of Materials*. 2014;**69**:195-203
- [21] M'Saoubi R, Johansson MP, Andersson JM. Wear mechanisms of PVD-coated PCBN cutting tools. *Wear*. 2013;**302**:1219-1229
- [22] Koseki S, Inoueb K, Usuki H. Damage of physical vapor deposition coatings of cutting tools during alloy 718 turning. *Precision Engineering*. 2016;**44**:41-54
- [23] Kumar S, Curtin WA. Crack interaction with microstructure. *Materials Today*. 2007;**10**(9):34-44
- [24] Hosseini-Toudeshky H, Hosseini S, Mohammadi B. Delamination buckling growth in laminated composites using layer wise-interface element. *Composite Structures*. 2010;**92**:1846-1856
- [25] Pascoe JA, Rans CD, Alderliesten RC, Benedictus R. Fatigue disbonding of bonded repairs—An application of the strain energy approach. 27th ICAF Symposium; 5–7 June 2013; Jerusalem

- [26] Pascoe JA, Rans CD, Benedictus R. Characterizing fatigue delamination growth behavior using specimens with multiple delaminations: The effect of unequal delamination lengths. *Engineering Fracture Mechanics*. 2013;**109**:150-160
- [27] Rybicki E, Kanninen M. A finite element calculation of stress intensity factors by a modified crack closure integral. *Engineering Fracture Mechanics*. 1977;**9**(4):931-938
- [28] Vereschaka AA, Grigoriev SN, Sitnikov NN, Batako A. Delamination and longitudinal cracking in multi-layered composite nano-structured coatings and their influence on cutting tool life. *Wear*. 2017;**390–391**:209-219. DOI: 10.1016/j.wear.2017.07.021
- [29] Johnson KL. *Contact Mechanics*. Cambridge: Cambridge University Press; 1985
- [30] Hertzberg RW. *Deformation and Fracture Mechanics of Engineering Materials*. New York: John Wiley & Sons; 1996
- [31] Gent AN, Mars WV. Strength of elastomers. In: Mark JE, Erman B, Roland M, editors. *The Science and Technology of Rubber*. 4th ed. Boston: Academic Press; 2013. pp. 473-516
- [32] Paris P, Gomez M, Anderson W. A rational analytic theory of fatigue. *The Trend in Engineering*. 1961;**13**:9-14
- [33] Rans CD, Alderliesten RC, Benedictus R. Misinterpreting the results: How similitude can improve our understanding of fatigue delamination growth. *Composites Science and Technology*. 2011;**71**:230-238
- [34] Hume-Rothery W. *Atomic Theory for Students of Metallurgy*. London: The Institute of Metals; 1969 (fifth reprint)
- [35] Oliver WC, Pharr GMJ. An improved technique for determining hardness and elastic modulus using load and displacement sensing indentation. *Journal of Materials Research*. 1992;**7**:1564-1583